Directional Wind Spectrum Description using Bivariate L₁ Norm RBFs

Dario Ban, Stipe Perišić, Jani Barle

Faculty of Electrical Engineering, Mechanical Engineering and Naval Architecture, University of Split, Split, REPUBLIC OF CROATIA
e-mails: darioban@fesb.hr; stipe.perisic@fesb.hr; barle@fesb.hr

SUMMARY

In this paper, the simplest directional wind spectrum description is given using surrogate bivariate polynomial radial basis functions (PRBF) with L_1 norm smoothed by dense boundary points distribution, which enables an accurate description of the geometry and the calculation of the volume below the observed surface when belonging double integral is known. For that purpose, the direct solution of double integral below the descriptive surface is given for bivariate polynomial RBFs with integer exponents, which is examined for accuracy on two examples, for Franke's 2D function and upper hemisphere. After proven accurate in those examples, the direct description of the directional wind spectrum and the calculation of the joint density function of the wind spectrum is done in the paper, thus proving PRBFs as an efficient method for wind spectrum description. In that way, it is possible to calculate the joint density function (JDF) of the actual measured directional wind spectrum analytically, instead of the theoretical calculations used so far.

KEYWORDS: *RBF interpolation; L_1 norm; analytical double integral solution; directional wind spectrum; joint density function.*

1. INTRODUCTION

Radial basis function neural networks (RBFNN) are a basic technique for solving geometry description problems based on meshless data organization. Their reconstruction properties make them useful in dealing with the global description of artificial objects of complex form, to rough data sets from various real-world measurements [1], [2], and [3]. Standard RBF definitions, mostly used in practice, contain Euclid's L_2 norm squared as an argument, in order to ensure positive definiteness connected with the invertibility of the interpolation matrix. Their applicability and computational properties have been investigated in theory by many authors, such as in [4] to [9], with belonging calculation improvements investigated in [10] for constructive L_2 RBF and machine learning in [11].

Since RBFs with L_2 norm have some special properties that make them favorable over other norms as RBF arguments, other norms like L_1 norm are not very much used or covered in theory.

Nevertheless, it is shown by Ban et al., [12], that global ship hull geometry description is possible using a single radial basis function based on the L_1 norm, showing their main property of geometry features extraction, since they don't suffer from fill distance limitations of data site points. That feature makes radial basis functions with L_1 norm applicable in directional wind spectrum description, as will be shown in this paper.

In order to solve the problem of smooth surface reconstruction problem for RBFs with L_1 norm, the smoothing method using dense points description of surface boundaries will be used in this paper, thus enabling surface description using RBF in polynomial form with integer exponents. Simultaneously, Runge phenomenon of boundary oscillations is reduced, which is investigated by many authors, like Fornberg and Zuev, [13], and Boyd, [14], who observed it in many ways with various solutions. Moreover, as it is shown in [15] and [16], complete analytical solutions to 2D computational geometry problems are available using the composition of cubic and linear Polynomial RBFs, solving Runge and Gibbs phenomena and intersection problem.

Consequently, RBF forms that will be used for describing directional wind spectrum surface S, obtained from measured histogram data, are those basis functions with the polynomial form with integer function exponents that could enable the direct solution of double integral below directional wind spectrum surface:

$$V = \int\limits_{0}^{2\pi} \int\limits_{0}^{v_{max}} f(\varphi,v)d\varphi dv \tag{1}$$

where φ is wind direction from 0 to 360°, and v is wind speed from 0 to v_{max}.

Therefore, the polynomial form of RBFs with integer main function exponent and L_1 norm as the argument will be examined in this paper, giving double integral under described surface S of the type shown below as:

$$\iint\limits_{S} f(|x-a|,|y-b|)dxdy \tag{2}$$

After solving double integral in (2), actual normalized joint density function (JDF), f_{XY}, for measured directional wind spectrum can be calculated by dividing surrogate L_1 norm RBF (L1RBF) directional wind spectrum description $f(\varphi, v)$, defined for wind direction φ and with speed v, with calculated volume V below spectrum surface as:

$$f_{XY} = \frac{f(\varphi,v)}{V} = \frac{f(\varphi,v)}{\int\limits_{0}^{2\pi} \int\limits_{0}^{v_{MAX}} f(\varphi,v)d\varphi dv} \tag{3}$$

The integration results of multiquadric and polynomial radial basis functions defined with L_1 norm will be first tested for theoretical Franke's function, [17], with a shape similar to the directional wind spectrum, then for the description of an ideal geometry of the upper hemisphere, and then applied in joint density function (JDF) calculation for actual directional wind spectrum.

2. RADIAL BASIS FUNCTIONS DEFINITION

2.1 GENERAL

Radial basis functions are the direct solution to scattered data interpolation problems with foundations in statistics, [18]. They were usually used as activation functions in direct feed-forward neural networks (FF-NN), but they are the basis of meshless methods, also, because they don't need mesh organization of their data site X, with belonging input data set equal $\{x_j\}$, $j = 1, ...,$ N, $x \in IR^d$, and output data set $\{z_j\}$, $j = 1, ..., N$, $z \in IR$. Their applicability in ship geometry description using global interpolation was explored in [19], where multiquadric RBFs (MQ RBF) were found useful for that purpose. In this paper, we are interested in a basis function $f: \Omega \rightarrow IR$ defined on some region $\Omega \subseteq IR^d$ where d is the dimension of the problem.

In general, the RBF statement can be described as a weighted sum of radial basis functions translated around the points t_i called centers, whose number depends on the mathematical procedure chosen for object representation. Mathematically, an RBF network as a linear combination of certain basis functions is defined with:

$$\hat{f}(x) = \sum_{i=1}^{O} w_i B_i = \sum_{i=1}^{O} w_i \Phi_i(x) = \sum_{i=1}^{O} w_i \varphi(\|x, t_i\|) \tag{4}$$

where $\{x_j\}$, $j = 1, ..., N$; $x \in IR^d$ is the input data set, $\{B_i\}$ are basis functions, $\{\Phi_i\}$ are radial basis functions, $\{t_i\}$ are RBF development centers, with $i = 1, ..., O$, where O is the number of centers, $\{w_i\}$ are RBF network weight coefficients, ϕ is radial basis function based on the Euclidian norm L_2 between input data and centers, and $\hat{f}(x)$ is generalized interpolation/approximation function.

The main advantage of RBFs is that they are the solution of scattered data interpolation problem that is obtained by determination of weight coefficient vector/matrix w, using inversion of interpolating matrix H as:

$$w = H^{-1} \cdot z \tag{5}$$

where $w = \{w_i\}$ is weight coefficients matrix/vector, $z = \{z_j\} \in IR$ is output data set with $j = 1, ..., N$, for belonging input data set as $x = \{x_{jd}\}$, $j = 1, ..., N$, $H = [H_{ji}]$ is interpolating matrix with elements $H_{ji} = \Phi\|x_j - x_i\|$, and d is the dimensionality of the problem.

Generalized multiquadric RBFs (MQ RBF), founded by Hardy, [24], are written in the form:

$$f(x; c; k) = \sum_i w_i \left\{ r_i^2 + c^2 \right\}^{\frac{k}{2}}, \ k \notin 2IN \tag{6}$$

where r is the L_2 norm, which can be written as: $r \equiv L_2 = \left[(x - x_i)^2 + (y - y_i)^2 \right]^{\frac{1}{2}}$.

It is obvious from (9) that r is squared in order to eliminate the $1/2$ exponent in the L_2 norm in the MQ RBF definition. It means that an additional auxiliary exponent $\gamma = 2$ is introduced in the RBF definition to reduce the square root in the MQ RBF definition. Therefore, a more general MQ RBF definition with auxiliary exponent γ can be written as:

$$f(r; c; k, \gamma) = \sum_i w_i \left(r_i^{\gamma} + c^{\gamma} \right)^{\frac{k}{2}}, \ k \notin 2 \cdot IN \tag{7}$$

Therefore, the main goal of all radial basis function selections is to ensure the inversion of the

global interpolating matrix **H**. Several RBF types are developed in theory with the main goal to have a positive definite radial basis with different function types: strictly positive definite, completely monotone, multiply monotone functions, and conditionally positive definite functions. For those classes of RBFs, the usual proposition is that they follow Schoenberg-Menger theorem, [20], and Micchelli's theorem, [21], which require an L_2 norm to be squared with L_2^2 to obtain conditionally positive semi-definite matrix and ensure its invertibility, in the form:

$$H_{ji} = \left\| \boldsymbol{x}_j - \boldsymbol{x}_i \right\|_2^2 \tag{8}$$

Moreover, the ball-in-the-cone condition can be fulfilled in such a way, but using the L_2 norm also leads to the main limitation of RBFs with L_2 norm i.e., the existence of fill distance between points $h_{X,\Omega}$ limitation in data site points arrangement. It means that data site X cannot be freely chosen for RBFs with L_2 norm, and that makes major difficulties in the description of geometries with discontinuities or limits integration with grouping error in a point effect for such descriptions.

The possibility of other norm choices was investigated by several authors, Baxter [22], and Dyn et al. [23], where the choice of L_1 norm proves to give a singular matrix for a very simple set of points for surface description problems, thus assuming elimination of possible usage of L_1 norm for RBF definitions. On the other hand, using the L_1 norm erases the limitation of the fill distance between points $h_{X,\Omega}$ for surface description problems, thus improving the convergence of the interpolation. It is also shown in Fasshauer, [20], and in Ban et al., [12], that the well-known problem of interpolation matrix inversion for simple data set $X = \{0\ 1,\ 0\ 1\}$ is possible for random choice of points or slight imperfection of results, as is usual for real geometries, and thus eliminating that problem.

2.2 RBF WITH L₁ NORM

2.2.1 GENERAL

Standard RBFs have an L_2 norm in order to ensure positive definiteness and invertibility of interpolation matrix H, and it can be achieved by squaring the L_2 norm only. This leads to the existence of fill distance between points $h_{X,\Omega}$ limitation in data site points arrangement as the greatest limitation of L_2 norm-based RBFs in the surface's reconstruction. On the other hand, when RBFs with L_1 norm are used to fill the distance between points $h_{X,\Omega}$ limitation does not exist with:

$$h_{X,\Omega} \to 0 \tag{9}$$

It means that the only necessary requirement for RBF interpolation with L_1 norm to be non-singular is that all points are distinguished from each other with:

$$X_1 \neq X_2 \neq X_3 \neq \ldots \neq X_{N-1} \neq X_N \tag{10}$$

Therefore, data site X used for the description of some arbitrary geometry with discontinuities can be freely chosen, with denser descriptions near discontinuities. That is one of the main reasons why RBFs with L_1 norm should be used, together with the possibility of obtaining RBFs in polynomial form. Except above, interpolation matrix H is much simpler than for L_2 norm, thus assuring invertibility and faster calculation. Moreover, in the case of polynomial RBFs with shape parameter c set to zero, the symmetric matrix is obtained with the main diagonal equal to zero, too. Also, it is shown by Ban & Basic in [16] that polynomial RBFs are directly integrable for 2D

computational geometry problems, and thus they are assumed to have an appropriate form for 3D computational geometry solutions, too.

Undesired absence of generalization smoothness for polynomial and multiquadric RBFs with L_1 norm and integer exponents leads to non-smooth and bumpy surface descriptions, that is solved by the dense distribution of boundary points, with two types of boundary points distributions examined: equally and randomly distributed points.

2.2.2 MQRBF WITH L₁ NORM

After reducing exponents and setting $\gamma = 1$, simpler multiquadric RBFs for curve and surface descriptions are obtained. This MQRBF form has a polynomial form significantly simpler than (7) above and will be examined for surface geometry descriptions. We can then write MQRBF with L_1 norm as:

$$f(\boldsymbol{x}) = \sum_{i=1}^{N} w_i \left(\left| \boldsymbol{x} - \boldsymbol{x}_i \right| + c \right)^{\beta} \tag{11}$$

Opposite to the multiquadric definition with L_2 norm squared L_2^2, where the choice of data site does not influence RBF definition, the choice of data site X for L_1 norm does influence the characteristics of RBF definition. Therefore, it is necessary to examine the influence of data site points distribution on RBF definitions.

According to theory, the MQ RBF definition for L_1 norm and equally distributed points is:

$$f(\boldsymbol{x}) = \sum_{i=1}^{N} w_i \left(\left| \boldsymbol{x} - \boldsymbol{x}_i \right| + c \right)^{\beta}, \ \beta \in IR^+ \backslash \{1\} \tag{12}$$

This fact is well described in theory, [21], where the linear multivariate description is not possible for equally distributed data points. Fortunately, that can be changed using a random distribution of data points X, where MQ RBF changes to:

$$f(\boldsymbol{x}) = \sum_{i=1}^{N} w_i \left(\left| \boldsymbol{x} - \boldsymbol{x}_i \right| + c \right)^{\beta}, \ \beta \in IR^+ \tag{13}$$

In this way, MQ RBF becomes applicable for solving double integral enabling usage of whole space of integer function exponents, $\beta \in IN$, when the non-equidistant distribution of input points is used.

The form of MQ RBF that will be used for further calculations will be:

$$f(\boldsymbol{x}) = \sum_{i} w_i \left(\left| x - x_i \right| + \left| y - y_i \right| + c \right)^{\beta} \tag{14}$$

2.2.2 POLYNOMIAL RADIAL BASIS FUNCTIONS WITH L₁ NORM

It is obvious from the above that it is possible to obtain MQ RBF in polynomial form. But, as the polynomial form is obtained anyway, there is no need for c to be included in the brackets, in (13). It is possible to leave shape parameter c out of the brackets, thus obtaining polynomial RBFs (PRBF) defined with L_1 norm. Regarding main function exponent β in MQ RBF with L_1 norm, it is assumed that PRBF has a computationally efficient and robust form too, together with high precision, as shown in [12].

Polynomial RBFs with L_1 norm are generally defined with:

$$f(\boldsymbol{x}) = \sum_{i=1}^{N} w_i |\boldsymbol{x} - \boldsymbol{x}_i|^{\beta} + c \qquad (15)$$

But, except for dimensionality d of the problem, the definition of polynomial radial basis functions depends on the distribution of input points also, as shown in [12]. So, in the case of equidistant points, PRBF definition is:

$$f(\boldsymbol{x}) = \sum_{i=1}^{N} w_i |\boldsymbol{x} - \boldsymbol{x}_i|^{\beta} + c \,, \beta \in IR \backslash (2 \cdot IN - s + 1) \qquad (16)$$

where $s = d - 1$.

It can be concluded from above that the reason for integer exponent values β to become acceptable for PRBFs is because they have L_1 norm, thus avoiding squaring of the norm as used in standard RBF definitions with L_2 norm, directed by Schoenberg-Menger's theorem for conditionally positive semi-definite matrices, [20], similar to MQ RBFs. Moreover, for known interpolation problem with the singularity of simple four equidistant points, described in [12] and [20], it can be decided easily that it emerges because of the definition of 3D PRBFs and its limitation to odd integer values, only, as shown in (16).

On the other hand, in the case of non-equidistant points, where low discrepancy Van der Corput sequences like in Halton points are used, the definition of the 3D PRBF changes to:

$$f(\boldsymbol{x}) = \sum_{i=1}^{N} w_i |\boldsymbol{x} - \boldsymbol{x}_i|^{\beta} + c \,, \beta \in IR^+ \qquad (17)$$

showing the dependence of the RBFs with the L_1 norm definition of the input data site.

Depending on the dimensionality of the problem, equation (17) can be rewritten for 2D and 3D as:

$$f(\boldsymbol{x}) = \sum_{i=1}^{N} w_i \left(|x - x_i| + |y - y_i| \right)^{\beta} + c \qquad (18)$$

where equation (18) represents the main function type in the double integral (1) to be solved.

Therefore, the polynomial RBFs (PRBF), together with multiquadric RBFs (MQ RBF), can have all integer exponents from space of natural numbers IN and can be used for direct analytical solving of computational geometry problems like double integrals. Nevertheless, arbitrary surface description using RBFs with L_1 norm usually suffers from poor generalization properties. It will be shown in the next section that can be improved by the dense distribution of boundary input points. The results will be then tested for 3D Franke's function and theoretical hemisphere in the next sections.

2.3 SURFACE TENSION USING DENSE DISTRIBUTION OF BOUNDARY POINTS

One of the simplest methods of surface smoothening is adding points at surface boundaries, as Ban & Ljubenkov have shown in [12], where the actual ship's hull form is described. Moreover, it is shown in [12] that smoothness of the surface description can be achieved using the global meshless description of hull form using single polynomial RBF with the dense distribution of the

input points on the boundaries of the description and at the inner discontinuities of the geometry. After adding boundary points, the number of points in input data set X changes to:

$$N = N_S + N_B + N_D \qquad \text{(19)}$$

where N_S is the number of points describing the smooth part of the description and N_B is the number of boundary points and N_D is the number of points used for the description of inner discontinuities.

In order to test the properties of radial basis functions with L_1 norm in the global 3D meshless description, modified 3D Franke's function with all positive values is described here. In that way, modified 3D Franke's function simulates directional wind spectrum characteristics that have all positive values, also. Two types of boundaries description are examined here for 3D Franke's function, described using MQ RBFs and PRBFs with $\beta = 2.0$ and $N_S = 1089$ points: with randomly and equally distributed boundary points, N_B. The results show that the accuracy of the description does not rise significantly with more boundary points added in the description, or after some number of added points N_B is reached, but a larger number of added boundary points give better smoothness of the description. Also, there is not much difference between the boundary points distribution chosen, i.e. the distribution of points does not influence the result significantly.
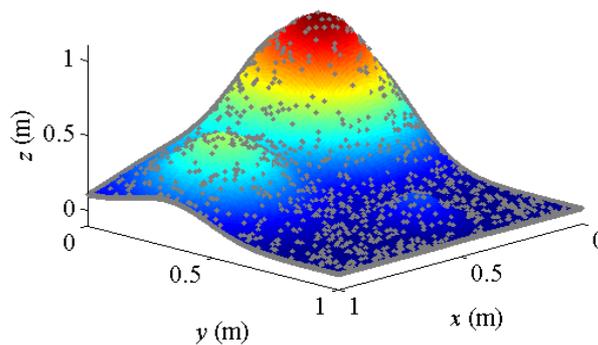
Fig. 1 *MQ RBF description of 3D Franke's function with L_1 norm, $\beta = 2.0$, and equidistant boundary points*

Figure 1 shows that an acceptable description regarding smoothness is obtained using dense boundary points distribution in the description of 3D Franke's function for MQ RBF with L_1 norm and exponent $\beta = 2.0$. Although the local accuracy value $Err_{max} = 5 \cdot 10^{-3}$ is good, it is not matching the required value of 10^{-3}. Regarding global accuracy, a very good value is obtained, with RMSE = $2.873 \cdot 10^{-6}$.

According to the above, multi quadrics and polynomial RBFs with L_1 norm have the simplest definition forms, and they will be suggested as the solution to 3D computational geometry problems with RBFs. They both have polynomial form when integer function exponent is applied and therefore could be easily integrated, i.e. the solution of respective double integral below the described surface should be obtained directly. Moreover, the simplest polynomial RBF that can be used for surface description is bivariate quadratic polynomial RBF with:

$$f(x) = \sum_{i=1}^{N} w_i |\boldsymbol{x} - \boldsymbol{x}_i|^2 + c \qquad \text{(20)}$$

This description, therefore, changes from C^2 to C^1, giving quasi-smooth interpolation, where smoothness is obtained using dense surface boundary description. Thus, polynomial RBFs with

integer exponent $\beta = 2.0$ can be used for solving double integral for volume calculation also, since they have a very simple definition.

3. ANALYTICAL SOLUTION OF DOUBLE INTEGRAL BELOW L1 NORM RBF SURFACE

For the complete analytical solution of the 3D computational geometry description problem, belonging to double integral must be solved, as well as appropriate smooth surface description achieved, simultaneously. It is shown in the previous section that a smooth description of surfaces can be obtained using RBFs with L_1 norm in polynomial form smoothed using dense surface boundary description. Therefore, multiquadric (MQ RBF) and polynomial (PRBF) radial basis functions are the best candidates for the solution of double integral below the surface. Among those two, MQ RBF has a more general form with shape parameter c included inside brackets with:

$$f(x,y) = \sum_i w_i \left(|x - x_i| + |y - y_i| + c \right)^\beta \tag{21}$$

Belonging definite double integral for MQRBF then simply represents volume V below-described surface bounded by $a \le x \le b$ and $d \le y \le e$.

$$V = \int_{y=d}^{y=e} \int_{x=a}^{x=b} \sum_i w_i \left(|x - x_i| + |y - y_i| + c \right)^\beta dx dy \tag{22}$$

In order to solve the above indefinite integral for the segment i, the single indefinite integral for variable x is to be solved first, in the form:

$$I_x = \int \left[|x - x_i| + c_y \right]^\beta dx \tag{23}$$

with $c_y = |y - y_i| + c$.

The general solution of integral in (23), for integer exponents, is:

$$I_x = \frac{1}{2(\beta+1)} \left[\left(-x + x_i + c_y \right)^{\beta+1} \left(sign\left(x - x_i \right) - 1 \right) + \left(x - x_i + c_y \right)^{\beta+1} \left(sign\left(x - x_i \right) + 1 \right) \right] \tag{24}$$

The simplest way to obtain the required double integral solution is using L_1 norm multiquadric RBF with $\beta = 2$, where the bivariate quadratic function is obtained as:

$$I_x = \int \sum_i w_i \left(|x - x_i| + c_y \right)^2 dx dy \tag{25}$$

Belonging solution for quadratic multiquadric function in (24) with $\beta = 2$ can be then obtained from (25) as:

$$I_x = \frac{1}{6} \left[\left(-x + x_i + c_y \right)^3 \left(sign\left(x - x_i \right) - 1 \right) + \left(x - x_i + c_y \right)^3 \left(sign\left(x - x_i \right) + 1 \right) \right] \tag{26}$$

The above solution for x, with substituting constant c_y and separating variable y, is then:

$$I_x = \frac{1}{6} \left[\left(-x + x_i + |y - y_i| + c \right)^3 \left(sign\left(x - x_i \right) - 1 \right) + \left(x - x_i + |y - y_i| + c \right)^3 \left(sign\left(x - x_i \right) + 1 \right) \right] \tag{27}$$

After that, it is necessary to integrate for y with basic integral having a similar form as the result for x in (26) with:

$$I_y = \int \left[\left| y - y_i \right| + c_1 \right]^3 dy \tag{28}$$

where $c_1 = -x + x_i + c$ for the first part of the solution in (28) and $c_1 = x - x_i + c$ in the second part.

The solution of the above integral (28), according to the solution in (24), is:

$$I_y = \frac{1}{8} \left[\left(-y + y_i + c_1 \right)^4 \left(sign\left(y - y_i \right) - 1 \right) + \left(y - y_i + c_1 \right)^4 \left(sign\left(y - y_i \right) + 1 \right) \right] \tag{29}$$

After replacing c_1 in (29), the overall solution of double integral below the surface for bivariate quadratic polynomial RBF, shape parameter c is not inside the brackets, and polynomial RBF can be taken as multiquadric RBF with $c = 0$. Therefore, c is zero for polynomial RBF and we obtain polynomial RBF that can be used for surface description as bivariate quadratic polynomial RBF, (20), with the simplest solution possible.

The final solution for bivariate quadratic polynomial RBF can be obtained as:

DOUBLE INTEGRAL SOLUTION FOR BIVARIATE QUADRATIC POLYNOMIAL RBF

$$
\begin{aligned}
I = \frac{1}{48} \sum_i w_i &\left[\left(sign\left(x - x_i \right) - 1 \right) \left(sign\left(y - y_i \right) - 1 \right) \left(-y + y_i - x + x_i \right)^4 \right. \\
&+ \left(sign\left(x - x_i \right) + 1 \right) \left(sign\left(y - y_i \right) - 1 \right) \left(-y + y_i + x - x_i \right)^4 \\
&+ \left(sign\left(x - x_i \right) - 1 \right) \left(sign\left(y - y_i \right) + 1 \right) \left(y - y_i - x + x_i \right)^4 \\
&\left. + \left(sign\left(x - x_i \right) + 1 \right) \left(sign\left(y - y_i \right) + 1 \right) \left(y - y_i + x - x_i \right)^4 \right]
\end{aligned}
\tag{30}
$$

Therefore, the direct solutions of double integral below the surface are obtained in the required polynomial form.

Finally, it is then necessary to insert the boundaries of volume double integral (22), and only the case for polynomial RBF will be shown here. If we observe the solution in (30), it is obvious that the sign function changes with center point values x_i. Nevertheless, if one widens boundaries of observed double integral $[x_a, x_b, y_a\ y_b]$ for some small value, let 's say $dX \equiv \{dx, dy\} \rightarrow 0$, one gets calculation area $[x_a - dx\ x_b + dx, y_a - dy\ y_b + dy]$.

In that way, the sign function reduces all parts of the integral solution (31) except one, for each combination of boundaries $x_a - dx, x_b + dx, y_a - dy, y_b + dy$, for the whole center point data set. As the result, the solution of definite integral (22), after inserting boundaries, becomes:

$$
\begin{aligned}
I = \frac{1}{48} \sum_i w_i &\left[4\left(-y_a + y_i - x_a + x_i + dx + dy \right)^4 + 4\left(-y_a + y_i + x_b - x_i + dx + dy \right)^4 \right. \\
&\left. + 4\left(y_b - y_i - x_a + x_i + dx + dy \right)^4 + 4\left(y_b - y_i + x_b - x_i + dx + dy \right)^4 \right]
\end{aligned}
\tag{31}
$$

And after reducing, the final solution is:

$$I = \frac{1}{12} \sum_i w_i \left[\left(-y_a + y_i - x_a + x_i + dx + dy \right)^4 + \left(-y_a + y_i + x_b - x_i + dx + dy \right)^4 \right.$$
$$\left. + \left(y_b - y_i - x_a + x_i + dx + dy \right)^4 + \left(y_b - y_i + x_b - x_i + dx + dy \right)^4 \right]$$

(32)

This solution of the double integral is used for further calculations in this paper.

4. RESULTS

Before giving directional wind spectrum description with belonging joint probability function, the accuracy of direct, analytical solution of double integral below the surface using 3D PRBF will be examined here, first, for two test examples: Franke's 3D function and upper hemisphere.

4.1 EXAMPLE 1: FRANKE'S 3D FUNCTION

The description of Franke's 3D function surface is a usual test for 3D reconstruction methods as described before. In order to show the possibilities of RBF description with L_1 norm function arguments, polynomial RBF results of integration (31) are examined here, and compared with direct solutions of 3D Franke's function double integral, in Table 1. Modified 3D Franke's function is used here as shown in Figure 1, with the last term added instead of subtracted defined as:

$$f_F(x,y) = 0.75 \cdot e^{\left[-\frac{(9x-2)^2}{4} - \frac{(9y-2)^2}{4} \right]} + 0.75 \cdot e^{\left[-\frac{(9x+1)^2}{49} - \frac{9y+1}{10} \right]} + 0.5 \cdot e^{\left[-\frac{(9x-7)^2}{4} - \frac{(9y-3)^2}{4} \right]} + 0.2 \cdot e^{\left[-(9x-4)^2 - (9y-7)^2 \right]}$$

After direct analytical integration, the solution of double integral for modified Franke's 3D function over integration area [0 1; 0 1] is 0.26072 (m³).

Table 1 shows the results regarding root mean square error (RMSE), maximal absolute error (Err_{max}), and volume below 3D Franke's function, described using smoothed polynomial RBF with L_1 norm and $\beta = 2$ with dense distribution of boundary points, for a range of input points N_S and additional equidistant boundary points N_B. As mentioned before, the calculation boundaries of the integration are widened for a small value to obtain the solution (34), to an area [0 – 10⁻¹⁰ 1 + 10⁻¹⁰, 0 – 10⁻¹⁰ 1 + 10⁻¹⁰].

Table 1 *Calculation results for Franke's 3D function description using polynomial RBF with L₁ norm*

N_S	N_B	Volume (m³)	RMSE	Err_{max}
1089	1000	0.26081	$6.000 \cdot 10^{-6}$	$9.596 \cdot 10^{-3}$
1089	1500	0.26072	$3.757 \cdot 10^{-5}$	$5.106 \cdot 10^{-3}$
1089	2000	0.26072	$1.694 \cdot 10^{-6}$	$5.674 \cdot 10^{-3}$
1089	2500	0.26067	$1.412 \cdot 10^{-6}$	$1.127 \cdot 10^{-2}$

It can be seen from Table 1, that calculated volume values using double integration of polynomial RBF, with exponent $\beta = 2$, are nearly equal to the volume value obtained by direct integration of Franke's 3D. Anyway, for values above $N_B = 3000$ additional points, the saturation of description occurs and no valid results are obtained, thus showing the limitation regarding the applicability of the used method.

4.2 EXAMPLE 1: UPPER HEMISPHERE

In order to further explore the possibilities of 3D PRBF volume calculation, the theoretical upper hemisphere surface is described here using polynomial RBF with L_1 norm and $\beta = 2$, and dense boundary description. After that, the belonging volume double integral is calculated and compared with the actual volume value. The belonging equation of the upper hemisphere of radius R is:

$$f(x, y) = (R^2 - x^2 - y^2)^{1/2}$$

The volume below an upper hemisphere surface can be determined directly, analytically with $V = 2/3 \cdot r^3 \cdot \pi$. Therefore, the volume of an upper hemisphere for the radius $R = 1$ is $V = 2/3 \cdot \pi = 2.0944$ (m^3).

The volume double integral solution for an upper hemisphere using quadratic polynomial RBF interpolation is then explored for various numbers of input points N_S and equidistant boundary and discontinuity points $N_B + N_D$, as shown in Table 2. The calculation boundaries in this example, are widened to the area $[-1 - 10^{-10}\ 1 + 10^{-10}, -1 - 10^{-10}\ 1 + 10^{-10}]$, in order to obtain a solution (32).

Table 2 *Calculation results for upper hemisphere with R = 1 using polynomial RBF with L_1 norm*

N_S	$N_B + N_D$	Volume (m^3)	RMSE	Err_{max}
1089	1000	2.0863	$2.081 \cdot 10^{-5}$	7.839
1089	2000	2.0973	$2.254 \cdot 10^{-6}$	0.159
1089	3000	2.0945	$9.489 \cdot 10^{-8}$	0.148
1089	4000	2.0968	$3.885 \cdot 10^{-7}$	0.109
1681	5000	2.0926	$4.383 \cdot 10^{-7}$	0.123
1681	6000	2.0944	$9.479 \cdot 10^{-5}$	0.113

The results of the double integral solution of an upper hemisphere described, using polynomial RBF with $\beta = 2$, L_1 norm and dense boundary description, in Table 2, shows very good agreement with an exact volume value for almost all combinations of input points N_S and $N_B + N_D$ points. Anyway, it can be seen from the above examples, that it is necessary to find appropriate relation between the number of N_S and $N_B + N_D$ points, in order to obtain the required surface description regarding the Err_{max} value.
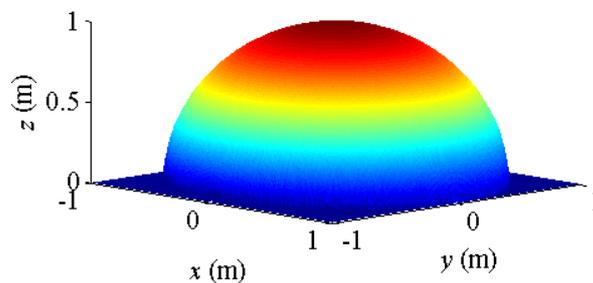
Fig. 2 *Upper hemisphere description using polynomial RBF with L_1 norm, $\beta = 2$, and $N_B + N_D = 6000$*

The description results can be inaccurate and either saturation can occur, or polynomial RBF description with $\beta = 2$ can have an undesired large local error value Err_{max}. But, for appropriate relation between input points N_S and $N_B + N_D$ boundary and discontinuity points, the results are excellent, with values matching exact ones as shown in Figure 2.

4.3 DIRECTIONAL WIND SPECTRUM JOINT DENSITY FUNCTION DESCRIPTION

It is shown in the previous sections that it is possible to describe various surface types using RBFs based on L_1 norm and boundary tension, with possibility of geometry features extraction. It is assumed also, that this description method will be efficient in wind spectrum description too, having all positive values of wind occurrence values shown on applicate axis, with possible calculation of joint density function (JDF), as described in (3).

In order to characterize the loading of wind turbines relevant physical quantities to be measured are various load quantities on blade, rotor and tower, operational parameters such as power, rotational speed, pitch angles, yaw position, azimuth angle, and meteorological parameters, as described in [25] and [26]. Nevertheless, meteorological parameters, such as wind speed and direction will be used for wind spectrum description here as in [27], thus enabling direct determination of site-specific wind load within an epoch, using discrete directional sectors/bins.

Usually, the description of actual directional wind spectrum surfaces is not possible using some surrogate representation technique. Therefore, theoretical statistical distributions are usually used instead in order to describe measured data. But, it is shown here that it is possible to do it using RBFs with L_1 norm and dense boundary description. The wind spectrum example shown here represents wind occurrence count binned with respect to speed and direction, measured during two days on Adriatic Sea coast, as shown in the Figure 3.

If we observe measured directional wind spectrum sequence in the Figure 3, it can be seen that it is typical one-peak spectrum with low ridge near 10 (*m/s*) wind speed, showing continuing wind direction change during one epoch. Since its data are binned, initial total data site has non-favorable equally distributed points that can produce computational problems. Because of that, not all data site points should be taken for wind spectrum description using RBFs with L_1 norm, and it is necessary to have random choice of calculation data site X points.
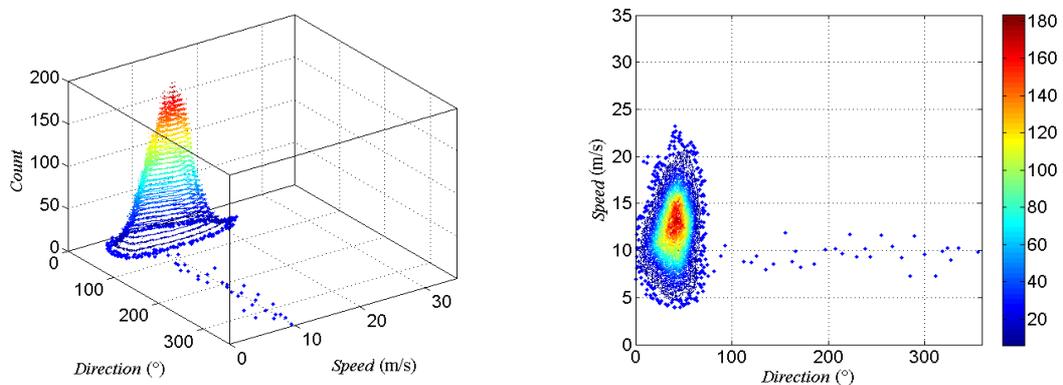
Fig. 3 *Actual directional wind spectrum*

That choice of the points distribution, together with smoothing using equidistant boundary points, further enables description of directional wind spectrum using RBFs with L_1 norm as shown below. Additionally, it is necessary to add randomly distributed near zero count points in empty areas in order to enable accurate description. Otherwise, non-wanted oscillations around zero count value could occur, and that need to be prevented for useful wind spectrum description.

The directional wind spectrum description using polynomial RBF with $\beta = 2$ and L_1 norm is shown in the Figure 4. In order to show description properties, displayed range is shortened from whole range of direction and wind speed values [0 360; 0 35] to [0 200; 0 25]. The gray dots designate

input data site points *X*, spread along the description range, together with dense boundary points set on all four description area edges that look like lines in the Figure 4.
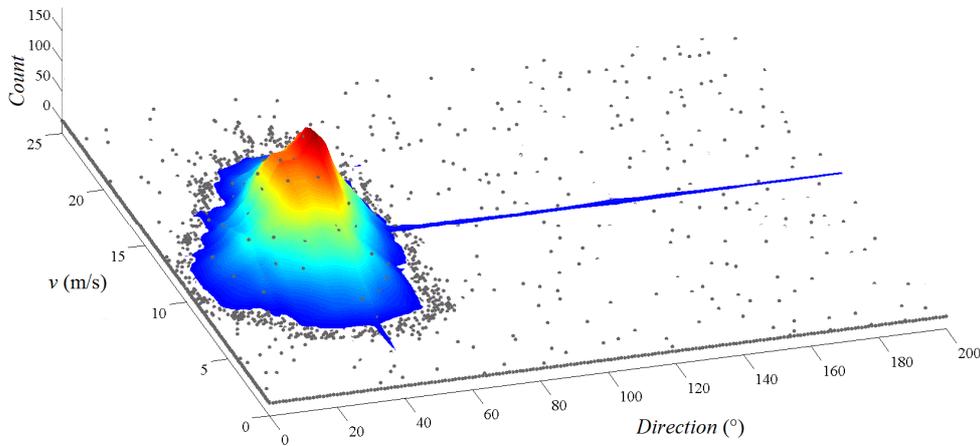
Fig. 4 *Directional wind spectrum described using polynomial RBF with β = 2.0 and L_1 norm*

It can be seen that the result of the description is satisfying regarding smoothness and accuracy, obtaining value of RMSE = $6.345 \cdot 10^{-5}$, with description of low ridge near 10 (*m/s*). Moreover, in the case of this test example, it is necessary to obtain all positive values of wind speed count number, i.e. the description need not oscillate below zero.

Negative description values are prevented with additional near zero points, giving total *N* = 2952 description points, that are consisting of initial N_S = 917 points and additional $N_B + N_D$ = 2035 boundary and discontinuity points. This number of points is relatively small considering total number of measured input points equal 360x360 points, but is necessary because quasi-interpolation method is used. In order to have larger number of points from measured data set, some of approximation description methods should be used, but that is not in the scope of this paper. Anyhow, directional wind spectrum approximation will be the topic of future work of the authors of this paper.

4.4 DIRECTIONAL WIND SPECTRUM JDF CALCULATION

One of the basic goals of some statistical data analysis is the calculation of the joint probability density function (JDF). When the wind spectrum is described using RBFs with L_1 norm, and surrogate surface function $f(\varphi, v)$ obtained, it is possible to solve the double integral below the wind spectrum surface using polynomial or MQ RBFs with integer exponent $\beta = 2$, as lowest possible polynomial radial basis function exponent when it is defined for L_1 norm. In that way, direct calculation of joint probability density function f_{XY} is becoming possible in the form shown in equation (3). Since polynomial RBF has a slightly simpler form, the volume below described directional wind spectrum surface *S* is calculated using that RBF with integer exponent $\beta = 2$.

For bivariate polynomial RBF with L_1 norm (L1RBF) and $\beta = 2$ equation (3) can be written as:

$$f_{XY} = \frac{\sum_{i=1}^{N} w_i \left(|\varphi - \varphi_i| + |v - v_i| \right)^2}{\int_0^{360} \int_0^{v_{MAX}} \left[\sum_{i=1}^{N} w_i \left(|\varphi - \varphi_i| + |v - v_i| \right)^2 \right] d\varphi \, dv} \tag{33}$$

where φ is the wind direction from [0, 360] and v is wind speed [0, 35].

The result of direct double integration using solution (32), for spectrum scaled to [0 1, 0 1], is then volume below surrogate surface description, that after rescaling equals $V = 36147.65$.

The joint probability density function (JDF) is then:

$$f_{XY} = \frac{f(\varphi,v)}{36147.65} = \frac{\sum_{i=1}^{N} w_i \left(|\varphi - \varphi_i| + |v - v_i| \right)^2}{36147.65} \tag{33}$$

In this way, the simplest solution to the JDF determination problem is obtained, using smoothed bivariate polynomial RBF with L_1 norm (L1RBF) and main function exponent $\beta = 2$. The directional wind spectrum can be scaled in time in that way, thus giving one more useful property of RBF description with L_1 norm under boundary tension. Moreover, such a normalized histogram represents smoothed probability density function, and it is easy to do its transformations for basic coordinates, with keeping basic properties.

5. CONCLUSION

The radial basis functions with L_1 norm (L1RBF) are novel quasi-smooth surface description methods based on the dense distribution of boundary input points, with function exponents β from the whole space of positive real numbers. Since polynomial and multiquadric RBFs have L_1 norm as a function argument, belonging data site used for surface description has no limitation regarding fill distance between input points, thus enabling geometric features extraction and accurate description of object boundaries.

The RBF descriptions with L_1 norm can be obtained in the required polynomial form too, with integer exponents of basis functions, $\beta \in IN$, that are enabling direct, analytical integration below some described surface, which has not been possible so far. Moreover, simple quadratic bivariate polynomial RBFs and multiquadric RBFs with L_1 norm can be obtained, thus having the lowest polynomial order for smooth surface description. This solution of smooth surface description, obtained with quadratic bivariate polynomial and multiquadric RBFs with L_1 norm using the dense distribution of boundary input points, is the simplest description method possible that enables the analytical solution of double integral, simultaneously.

Nevertheless, more complex geometries and some quadratic surfaces cannot be described using integer exponents with polynomial and multiquadric RBFs. Therefore, their double integral will not have a polynomial form, and that solution is to be found separately.

Besides application for directional wind spectra description, it is assumed that the description method using radial basis functions with L_1 norm as an argument and dense distribution of boundary input points will have application in computational geometry applications in general, and that will be investigated in further work of the authors of this paper. directional wind spectrum approximation using radial basis functions with L_1 norm will be investigated as well, and possible advantages of that type of description over interpolation will be examined.

6. REFERENCES

[1] D. Lowe, M. Tipping, Feed-forward neural networks and topographic mappings for exploratory data analysis, *Neural Computing and Applications*, Vol. 4, No. 2, pp. 83-95, 1996.

https://doi.org/10.1007/BF01413744

[2] M.M. Li, B. Verma, X. Fan, K. Tickle, RBF neural networks for solving the inverse problem of backscattering spectra, *Neural Computing and Applications*, Vol. 17, No. 4, pp. 391-397, 2008. https://doi.org/10.1007/s00521-007-0138-2

[3] H. Liao, S. Ding, M. Wang, G. Ma, An overview on rough neural networks, *Neural Computing and Applications*, Vol. 27, pp. 1805-1816, 2016.

https://doi.org/10.1007/s00521-015-2009-6

[4] M.D. Buhmann, *Radial Basis Functions*, Theory and Implementations, Cambridge Monographs on Applied and Computational Mathematics 12, Cambridge University Press, 2003. https://doi.org/10.1017/CBO9780511543241

[5] H. Wendland, *Scattered Data Approximation*, Cambridge University Press, 2005.

https://doi.org/10.1017/CBO9780511617539

[6] R. Schaback, H. Wendland, Kernel techniques: from machine learning to meshless methods, *Acta Numerica*, Vol. 15, pp. 543-639, 2006.

https://doi.org/10.1017/S0962492906270016

[7] E. Larson, B. Fornberg, Theoretical and computational aspects of multivariate interpolation with increasingly flat radial basis functions, *Computers and Mathematics with Application*, Vol. 49, Iss. 1, pp. 103-130, 2005. https://doi.org/10.1016/j.camwa.2005.01.010

[8] G. Casciola, D. Lazzaro, L.B. Montefusco, S. Morigi, Shape preserving surface reconstruction using locally anisotropic radial basis function interpolation, *Applied and Computational Mathematics*, Vol. 51, Iss. 8, pp. 1185-1198, 2006.

https://doi.org/10.1016/j.camwa.2006.04.002

[9] R.B. Platte, T.A. Driscoll, Polynomials and potential theory for Gaussian radial basis function interpolation, *SIAM Journal on Numerical Analysis*, Vol. 43, Iss. 2, pp. 750-766, 2005.

https://doi.org/10.1137/040610143

[10] H. Muzhou, H. Xuli, Multivariate numerical approximation using constructive L2(R) RBF neural network, *Neural Computing and Applications*, Vol. 21, No. 1, pp. 25-34, 2012.

https://doi.org/10.1007/s00521-011-0604-8

[11] Z.H. Zhou, J.W. Zhao, F.L. Cao, Surface reconstruction based on extreme learning machine, *Neural Computing and Applications*, Vol. 23, No. 2, pp. 283-292, 2013.

https://doi.org/10.1007/s00521-012-0891-8

[12] D. Ban, B. Ljubenkov, Global ship hull description using single RBF, *Towards Green Marine Technology and Transport* – Guedes Soares, Dejhalla, Pavletić, (Eds.), Taylor & Francis Group, London, pp. 457-464, 2015.

[13] B. Fornberg, J. Zuev, The Runge phenomenon and spatially variable shape parameters in RBF interpolation, *Applied and Computational Mathematics*, Vol. 54, Iss. 3, pp. 379-398, 2007. https://doi.org/10.1016/j.camwa.2007.01.028

[14] J.P. Boyd, Six strategies for defeating the Runge phenomenon in Gaussian radial basis functions on a finite interval, *Applied and Computational Mathematics*, Vol. 60, Iss. 12, pp. 3108-3122, 2010. https://doi.org/10.1016/j.camwa.2010.10.015

[15] D. Ban, B. Blagojević, B. Čalić, Analytical solution of global 2D description of ship geometry with discontinuities using composition of polynomial radial basis functions, *Brodogradnja*, Vol. 65, No. 2, pp. 1-22, 2014.

[16] D. Ban, J. Bašić, Analytical solution of basic ship hydrostatic integrals using polynomial radial basis functions, *Brodogradnja*, Vol. 66, No. 3, pp. 15-37, 2015.

[17] R. Franke, Scattered Data Interpolation: Tests of Some Methods, *Mathematics of Computation*, Vol. 38, pp. 181-200, 1982.

https://doi.org/10.1090/S0025-5718-1982-0637296-4

[18] D. Shepard, A two-dimensional interpolation function for irregularly spaced data, ACM '68: Proceedings of the 1968 23rd ACM National Conference, pp. 517 – 524, 1968.

https://doi.org/10.1145/800186.810616

[19] D. Ban, B. Blagojević, J. Barle, Ship geometry description using global 2D RBF interpolation, *Brodogradnja*, Vo. 61, No. 3, pp. 233-242, 2010.

[20] G.E. Fasshauer, *Meshfree Approximation Methods with MATLAB*, Interdisciplinary Mathematical Sciences - Vol. 6, World Scientific Publishers, Singapore, 2007.

https://doi.org/10.1142/6437

[21] C.A. Micchelli, Interpolation of scattered data: Distance matrices and conditionally positive definite functions, *Constructive Approximation*, Vol. 2, pp. 11-22, 1986.

https://doi.org/10.1007/BF01893414

[22] B.J.C. Baxter, Conditionally positive functions and p-norm distance matrices, *Constructive Approximation*, Vol. 7, pp. 427-440, 1991. https://doi.org/10.1007/BF01888167

[23] N. Dyn, W.A. Light, E.W. Cheney, Interpolation by piecewise-linear radial basis functions, *International Journal of Approximation Theory*, Vol. 59, Iss. 2, pp. 202-223, 1989.

https://doi.org/10.1016/0021-9045(89)90152-4

[24] R.L. Hardy, Multiquadric equations of topography and other irregular surfaces, *Journal of Geophysical Research*, Vol. 76, Iss. 8, pp. 1905-1915, 1971.

https://doi.org/10.1029/JB076i008p01905

[25] J. Holmes, *Wind Loading of Structures*, 2nd ed. Taylor & Francis, CRC press, ISBN: 0415409462, 2007. https://doi.org/10.4324/9780203964286

[26] EN 61400:2005 - Wind turbine generator systems – Part 01: Design requirement.

[27] M.P. Repetto, G. Solari, Directional wind-induced fatigue of slender vertical structures, *Journal of Structural Engineering-ACSE*, Vol. 130, Iss. 7, pp. 1032-1040, 2004.

https://doi.org/10.1061/(ASCE)0733-9445(2004)130:7(1032)